

7901-EN-01  
DTIC.

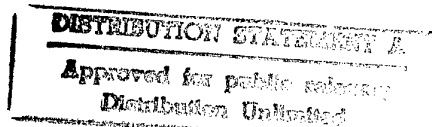
## The optical properties of aerosols

Final Technical Report  
by  
F. Borghese  
September 1997

United States Army  
EUROPEAN RESEARCH OFFICE OF THE U. S. ARMY  
London, England

Contract number N68171-96-C-9056  
Contractor: Centro Siciliano per le Ricerche Atmosferiche  
e di Fisica dell'Ambiente

Approved for public release; distribution unlimited.



19971112 073

**The optical properties of aerosols**  
Final Technical Report on Contract N68171-96-C-9056  
September 1997

The research performed under the present contract has dealt with the following items:

- 1) Optical properties of inclusion-containing hemispheres deposited on a perfectly reflecting surface.
- 2) Optical resonances of homogeneous spheres containing an eccentric spherical inclusion.
- 3) Optical properties of aggregated spheres deposited on a dielectric surface.

These researches are fully expounded in papers that have already been submitted for publication or are in an advanced stage of completion. Therefore, in the present report, we outline the motivations behind each work and summarize the main results.

**1) Optical properties of inclusion-containing hemispheres deposited on a perfectly reflecting surface.** The aim of this research is the assessment of the extent to which the presence of inclusions modify the scattering pattern from otherwise homogeneous hemispheres deposited on a perfectly reflecting surface. The practical interest of this kind of work is easily understood when one thinks of the hemispheres as liquid droplets deposited on a metallic surface and containing small pollutant particles. In this respect let us recall that a perfectly reflecting surface is the widely accepted model for a metal surface.

In performing our task we took advantage of our previous experience in the study of the optical properties, and in particular of the optical resonances, of single and aggregated homogeneous hemispheres deposited on a metallic surface. Indeed the technique that we used, both in our previous and in the present research is based on Image Theory, that, for the case of a perfectly reflecting surface, yields particularly simple and effective computational procedures. In fact, we were able to calculate, without undue computational effort, the pattern of the scattered intensity as a function of the angle of observation for several choices of the angle of incidence and of the polarization of the incident wave. Several morphologies were considered such as hemispherical and spherical inclusions as well as aggregations of two identical spheres. The polarization-dependent patterns proved useful to get information on the possible anisotropy of the inclusions, whereas the patterns obtained for different choices of the angle of incidence give information on the position of the inclusions within the host hemispheres.

Ultimately, the calculated patterns give enough information as to allow us to draw reliable conclusions both on the morphology and on the position of the inclusions. Therefore we plan to extend this work to include averages both over the position and the orientation of the inclusions in order to get information that may be of more direct use to the interested experimentalists.

**2) Optical resonances of homogeneous spheres containing an eccentric spherical inclusion.** The study of the optical resonances has proven to be a reliable method to get information on the internal structure of small particles. Nevertheless, the interpretation of the experimental data can be based on general grounds only for spheres either homogeneous or radially non homogeneous. For such objects, indeed, as a consequence of the spherical symmetry, the resonances do not depend either on the direction of incidence or on the polarization of the incident light. For non spherical particles the resonance spectra are rather more complicated, as the lack of spherical symmetry, implies a dependence of the resonance peaks both on the direction of incidence and on the polarization. Up today no general theory exists on which the interpretation of the observed spectra can be reliably based. For this reason a theoretical study of the behavior of the resonances of objects lacking the spherical symmetry may be of interest. Our research on the resonances deals with the calculation of the extinction spectrum from homogeneous spheres containing a spherical inclusion that is allowed to move from a concentric to an eccentric position. This case is of interest because the calculated spectra permit to follow the behavior of the resonance peaks when the symmetry of the scatterer as a whole lowers from spherical to cylindrical. Our actual calculations were performed on homogeneous spheres of MgO containing an inclusion of solid Mg; in other words we considered a metallic sphere (possibly eccentrically) coated by its oxyde.

As expected on the ground of Group Theory we found that the resonances undergo a splitting when the symmetry lowers. The splitting persists even when one considers the resonances from a dispersion of randomly oriented scatterers. When the latter spectrum is compared with those for a dispersion of likely oriented objects we found that it is possible to get information on the fraction of scatterers that are likely oriented. It is clear that such a possibility may be of help to study those processes that imply the orientation of anisotropic particles by electric or magnetic fields.

**3) Optical properties of aggregated spheres deposited on a dielectric surface.** Image theory proved in time to be the method of choice for the description of the optical properties of particles in the vicinity of a perfectly reflecting surface. Nevertheless, when the surface is a dielectric one, i. e. when it separates two different media, the choice of a different approach is in order. Indeed, several papers showed that, in the latter case, image theory yields a complicated procedure unless suitable approximations or assumptions on the size of the particles are made. Our Group, working under the preceding Contract was able to formulate a general theory for the reflection of vector multipole fields of arbitrary multiplicity, on a dielectric surface. This theory has then been applied to the description of the scattering properties of spheres, not necessary small, in the vicinity of a dielectric surface. The results obtained through our approach proved to be in excellent agreement with the results of ab initio simulations and with the experimental data so that we were encouraged to extend our method to describe the scattering properties of aggregated spheres. In this sense our present

research is a continuation of the work performed under the preceding Contract. The motivations that led us to perform this kind of extension are easily understandable. It is well known, indeed, that the solid particles in many aerosols may aggregate to form bigger particles that tend to fall under the effect of gravity and to deposit on any suitable surface. A reliable computational method that allows to foresee the changes undergone by a clean dielectric surface when aggregated particles are deposited is thus of interest.

The formulation of our theory is such as to permit to perform orientational averages over the particles and thus to describe the situation that is likely to occur in actual experiments. Nevertheless, due to the mathematical complications arising from the need to describe aggregated spheres, our calculations are not yet complete. We can state, however, that the preliminary result show the correct limiting behavior when the surface tends to become perfectly reflecting as well as when the interparticle interaction tend to weaken with increasing interparticle distance.

To complete this Report we include the preprint of the paper "Optical resonances of spheres containing an eccentric spherical inclusion" that has been submitted to Journal of Optics as well as reprints of the papers that have been published in the present year although performed under the preceding Contract.

# Optical resonances of spheres containing an eccentric spherical inclusion

F Borghese†, P Denti†, R Saija†, M A Iati† and O I Sindoni‡

† Università di Messina, Dipartimento di Fisica della Materia e Tecnologie Fisiche Avanzate and Istituto Nazionale di Fisica della Materia, sezione di Messina, Salita Sperone 31, 98166 Messina, Italy

‡ Edgewood Research Development Engineering Center, Aberdeen Proving Ground, Md 21010, U S A

**Abstract.** The resonance spectrum of small spheres of Mg with a spherical coating of MgO is calculated in the framework of the transition matrix approach. The spectrum for concentric coating displays a single resonance peak whereas when the coating is eccentric the spectrum complicates as the number of resonances increases. In the latter case, the spectrum undergoes evident qualitative changes according to the choice of the polarization. Comparison of the spectra for a dispersion of particles oriented alike with the one for randomly oriented particles suggests a possible procedure to evaluate the fraction of particles that are likely oriented.

PACS numbers: 42.25.Fx, 42.68.Mj

Short title: Resonances of eccentrically coated spheres

September 4, 1997

Submitted to "Journal of Optics" -

## 1. Introduction

The optical resonances of spherical particles have been thoroughly investigated both experimentally and theoretically [1, 2, 3, 4, 5] as they can give useful information e. g. on the nature and on the size of this kind of scatterers. The resonances may give useful information even for non spherical particles because the resonant behavior is expected to be strongly dependent on morphology as well as on the orientation of the particles with respect to the incident field.[6, 7] For instance, the literature reports studies intended to investigate the suppression of some of the resonances in the spectrum of axially symmetric particles for particular choices of the direction of incidence and of the polarization of the incident wave.[8, 9]

Among the methods that are applicable to calculate the extinction spectrum of particles, the transition matrix approach [10] plays a prominent role. Indeed, the related formalism, together with the theory of the vector multipole fields,[11] allows for the separation of the effects that are due to the morphology of the particles from the effects that are due to their orientation with respect to the incident field. As a result it becomes an easy matter to perform analytical angular averages so as to get information on the optical behavior of low-density dispersions with known, or assumed, distribution of the orientations of the particles.[12] Such averaging technique has been applied to calculate the extinction spectrum from dispersions both of aggregates of spherical scatterers and of homogeneous spheres containing spherical inclusions.[12, 13, 14] As individual scatterers the latter are particularly interesting because they may well appear as spherically symmetric but their calculated spectrum displays a noticeable dependence on the polarization and on the direction of the incident field. Even in the simple case of spheres containing a single inclusion, a calculation of the optical resonances may be useful to put into evidence the kind of the changes undergone by the spectrum when the inclusion occupies more and more eccentric positions. More precisely, such calculations may help to assess whether an experimental resonance spectrum may be effective to probe the internal asymmetry that is due to the eccentricity of the inclusion as well as to give indication on the fraction of the scattering particles that are likely oriented.

With this in mind, the present paper is devoted to the calculation of the extinction spectrum of a homogeneous sphere of MgO containing a spherical inclusion of Mg for a few different positions from the centered to the most eccentric one. Our choice of the material is not accidental as metal particles eccentrically coated by their oxyde are interesting e. g. in astrophysics as their presence in the interstellar dust is invoked to explain the observed dependence on the polarization of the galactic extinction.[15] The electromagnetic scattering properties of this kind of particles are calculated by resorting to the technique of Refs. [12, 13, 14]. Both the incident and the scattered field as well as the field within the particle are described through the appropriate expansions in terms

of vector multipole fields whose amplitudes are determined by the boundary conditions across the surface of each component of the scatterer. In fact, this procedure enables us to calculate the transition matrix as a function of the position of the inclusion, then the scattered field for given polarization and direction of incidence of the incoming field. Furthermore, by resorting to the well defined transformation properties of the multipole fields under rotation, we perform an average over the angular distribution of the particles to get information on the resonant behavior of a dispersion of particles.

In Section 2 we introduce the multipole expansion of the electromagnetic field and define the elements of the scattering amplitude in terms of the transition matrix elements and of the multipole amplitudes of the incident field.

In Section 3 we present the results of our calculation of the extinction efficiency of a dielectric sphere of MgO containing a spherical inclusion of Mg.

A few concluding remarks will be drawn in Section 4.

## 2. Transition matrix and scattering amplitude

We partition the space into the three regions sketched in Fig. 1: the external region, that is assumed to be filled by a homogeneous, non-dispersive, non-absorbing medium with refractive index  $n$  (typically the vacuum); the interstitial region, centered at the origin and of radius  $\rho_0$ , that is filled with a homogeneous, possibly dispersive and absorbing medium with refractive index  $n_0$ ; the region within the inclusion, centered at  $\mathbf{R}_1$  and of radius  $\rho_1$ , characterized by a refractive index  $n_1$  that may be dispersive and absorbing. For the sake of simplicity, the theory in this section will refer to homogeneous inclusions only, on account that the resulting formulas are easily extended to the case of radial nonhomogeneity.[17]

We assume that all the fields depend on time through the factor  $e^{-i\omega t}$  and define the propagation constants

$$K = kn, \quad K_0 = kn_0, \quad K_1 = kn_1,$$

in each of the regions mentioned above, respectively, with  $k = \omega/c$ . The incident field is assumed to be the plane wave of amplitude  $E_0$

$$\mathbf{E}_{I\eta} = E_0 \hat{\mathbf{u}}_{I\eta} e^{i\mathbf{K}_I \cdot \mathbf{r}},$$

where  $\mathbf{K}_I = K \hat{\mathbf{k}}_I$  is the incident wavevector;  $\hat{\mathbf{u}}_{I\eta}$  is a unit polarization vector whose index  $\eta$  indicates whether the field is parallel ( $\eta = 1$ ) or perpendicular ( $\eta = 2$ ) to the plane of scattering, i. e. to the plane that contains both  $\mathbf{K}_I$  and the direction of observation. The unit vectors  $\hat{\mathbf{u}}_{I\eta}$  are so oriented that

$$\hat{\mathbf{u}}_{I1} \times \hat{\mathbf{u}}_{I2} = \hat{\mathbf{k}}_I.$$

Since our approach makes extensive use of the multipole expansion of the electromagnetic field, let us define the multipole fields  $\mathbf{H}_{LM}^{(p)}$  as

$$\begin{aligned}\mathbf{H}_{LM}^{(1)}(\mathbf{r}, K) &= h_L(Kr) \mathbf{X}_{LM}(\hat{\mathbf{r}}), \\ \mathbf{H}_{LM}^{(2)}(\mathbf{r}, K) &= \frac{1}{K} \nabla \times \mathbf{H}_{LM}^{(1)}(\mathbf{r}, K).\end{aligned}\quad (1)$$

where the functions  $\mathbf{X}_{LM}$  are vector spherical harmonics [18] and, on account of the chosen time dependence of the fields, the quantities  $h_L$  are spherical Hankel functions of the first kind; the superscript  $p$  is a parity index that distinguishes the magnetic multipoles ( $p = 1$ ) from the electric ones ( $p = 2$ ). We also need to define the multipole fields  $\mathbf{J}_{LM}^{(p)}$  that are identical to the fields  $\mathbf{H}_{LM}^{(p)}$ , Eq. (1), except for the substitution of the spherical Bessel functions,  $j_L$ , in place of the Hankel functions,  $h_L$ .

The multipole expansion of the interstitial field as well as of the field within the inclusion are fully described in ref. [13]. Here we report only the expansion of the field in the external region where it is the superposition of the incident and of the scattered field and is, accordingly, expanded as

$$\mathbf{E}_\eta = \mathbf{E}_{S\eta} + \mathbf{E}_{I\eta} = E_0 \sum_{p, l, m} \left\{ A_{\eta l m}^{(p)} \mathbf{H}_{l m}^{(p)}(\mathbf{r}, K) + W_{l m}^{(p)}(\hat{\mathbf{u}}_{I\eta}, \hat{\mathbf{k}}_I) \mathbf{J}_{l m}^{(p)}(\mathbf{r}, K) \right\}.$$

The multipole amplitudes of the field scattered by the whole object,  $A_{\eta l m}^{(p)}$ , are expected to depend both on the polarization and on the direction of incidence as well as on the position of the inclusion within the external sphere. The quantities  $W_{l m}^{(p)}$  are the multipole amplitudes of the incident field that for a plane wave with polarization along the unit vector  $\hat{\mathbf{u}}$  are defined as [9, 12]

$$\begin{aligned}W_{LM}^{(1)}(\hat{\mathbf{u}}, \hat{\mathbf{k}}) &= 4\pi i^L \hat{\mathbf{u}} \cdot \mathbf{X}_{LM}(\hat{\mathbf{k}}), \\ W_{LM}^{(2)}(\hat{\mathbf{u}}, \hat{\mathbf{k}}) &= 4\pi i^{L+1} (\hat{\mathbf{k}} \times \hat{\mathbf{u}}) \cdot \mathbf{X}_{LM}(\hat{\mathbf{k}}).\end{aligned}\quad (2)$$

The amplitudes  $A_{\eta l m}^{(p)}$  are the main unknowns of the problem and are determined by boundary conditions at the surface of the inclusion as well as at the surface of the external sphere. The procedure for calculating the  $A$ -amplitudes is fully described in Ref. [13]. For our present purposes we only need to recall that the  $W$  and the  $A$ -amplitudes are related by the equation

$$A_{\eta l m}^{(p)} = \sum_{p' l' m'} S_{l m, l' m'}^{(p, p')} W_{l' m'}^{(p')}(\hat{\mathbf{u}}_{I\eta}, \hat{\mathbf{k}}_I), \quad (3)$$

where the quantities  $S_{l m, l' m'}^{(p, p')}$  are the elements of the so called transition matrix  $S$ , that accounts for the morphology (geometry and scattering power) of the particle. [10] Equation (3) shows that the resonances occur when, with varying frequency of the incident wave, at least one of the elements of  $S$  becomes much larger than any other element.[19] As a result some of the amplitudes  $A_{\eta l m}^{(p)}$  become large thus yielding a resonance peak that, for a given polarization,  $\eta$ , can be classified by the labels  $p$ ,  $l$ , and

*m.* Nevertheless, however large the elements of  $S$  may be, no resonance may occur if the appropriate amplitudes  $W_{\eta lm}^{(p)}$  in the expression of the incident field are vanishing.

The explicit expression of the transition matrix for a sphere containing an eccentric inclusion can be easily obtained by solving formally Eqs. (6) and (7) of Ref. [13]. The result is

$$S = (M_0 - M_W l_{0 \leftarrow 1} R_1 l_{1 \leftarrow 0})(R_0^{-1} - R_W l_{0 \leftarrow 1} R_1 l_{1 \leftarrow 0})^{-1}. \quad (4)$$

The elements of the matrices in the right hand side of Eq. (5) are explicitly given in Ref. [13]. All these matrices are diagonal except for  $l_{0 \leftarrow 1}$  and  $l_{1 \leftarrow 0}$  that account for the eccentricity of the inclusion: As a result  $S$  is a non-diagonal matrix. Nevertheless, in order to get a simpler expression for the transition matrix we assume that the diameter along which the center of the inclusion lies coincides with the  $z$  axis. With this choice of the geometry, in fact, the cylindrical symmetry around the  $z$  axis makes the elements of  $S$  to vanish for  $m \neq m'$ . Accordingly, they will be hereafter indicated as  $S_{l,l';m}^{(p,p')}$  and Eq. (3) takes on the simpler form

$$A_{\eta lm}^{(p)} = \sum_{p' l'} S_{l,l';m}^{(p,p')} W_{\eta l'm}^{(p')}. \quad (5)$$

It may be useful to remark that when  $R_1 \rightarrow 0$ , i. e. when the inclusion is centered, the scatterer becomes spherically symmetric and its transition matrix becomes diagonal with elements independent of  $m$ . In fact, it may be easily verified that the limiting expression of the matrix  $S$  coincides with the expression that is appropriate for a sphere containing a concentric inclusion.[20]

As usual, we describe the scattered field in the far zone through the normalized scattering amplitude  $f_\eta$  that is defined by the equation [18]

$$\mathbf{E}_{S\eta} = E_0 \frac{\exp(inkr)}{r} f_\eta(\mathbf{k}_I, \mathbf{k}_S).$$

The arguments of  $f_\eta$  recall that, in general, the scattering amplitude depends both on the incident and on the observed wavevector as well as on the polarization,  $\eta$ , of the incident field. In terms of the amplitudes of the scattered field the expression of  $f_\eta$  is [13]

$$\mathbf{f}_\eta = \frac{1}{K} \sum_{lm} (-i)^{l+1} [A_{\eta lm}^{(1)} \mathbf{X}_{lm}(\hat{\mathbf{k}}_S) + i A_{\eta lm}^{(2)} \hat{\mathbf{k}}_S \times \mathbf{X}_{lm}(\hat{\mathbf{k}}_S)], \quad (6)$$

where  $\hat{\mathbf{k}}_S$  denotes the direction of observation. Of course, the scattered field is neither parallel nor perpendicular to the plane of scattering: It can be decomposed, however, into its components that are parallel and perpendicular to this plane by projecting  $\mathbf{f}_\eta$  on the pair of unit vectors  $\hat{\mathbf{u}}_{S\eta}$  such that  $\hat{\mathbf{u}}_{S2} \equiv \hat{\mathbf{u}}_{I2}$  and

$$\hat{\mathbf{u}}_{S1} \times \hat{\mathbf{u}}_{S2} = \hat{\mathbf{k}}_S.$$

These vectors form the polarization basis that is appropriate for the scattered wave. The components of  $\mathbf{f}_\eta$  along these vectors turn out to be given by the equation

$$\begin{aligned} f_{\eta\eta'} &= \mathbf{f}_\eta \cdot \hat{\mathbf{u}}_{S\eta'} \\ &= -\frac{i}{4\pi nk} \sum_{pl} \sum_{p'l'} \sum_m W_{lm}^{(p)*}(\hat{\mathbf{u}}_{S\eta'}, \hat{\mathbf{k}}_S) S_{l,l';m}^{(p,p')} W_{l'm}^{(p')}(\hat{\mathbf{u}}_{I\eta}, \hat{\mathbf{k}}_I) \\ &= \sum_l B_{\eta\eta'l}, \end{aligned} \quad (7)$$

that is easily obtained from Eq. (6) with the help of Eqs. (2) and (5). The  $2 \times 2$  matrix of elements  $f_{\eta\eta'}$  has been used by van de Hulst [21] to illustrate the symmetry properties of a general scattering process. In particular, these symmetry properties, when considered together with the cylindrical symmetry of the scatterer, imply that  $f_{\eta\eta'} = 0$  when  $\eta \neq \eta'$ , viz. the scatterers we are dealing with here never give rise to cross-polarization effects.

Equation (7) shows that  $f_{\eta\eta'}$  depends not only on the properties of the transition matrix  $S$  but also on the properties of the  $W$ -amplitudes. In order to simplify our considerations we assume that the plane of scattering coincide with the  $x$ - $z$  plane; this choice, however does not imply any loss of generality because choosing any other plane through the  $z$  axis will only introduce an inessential phase factor. Now, with the help of the definition of the  $W$ -amplitudes, Eq. (2), it is an easy matter to prove that

$$W_{l'm}^{(p)}(\hat{\mathbf{u}}_{I\eta}, \hat{\mathbf{k}}_I) = (-)^{\eta+p+m-1} W_{l-m}^{(p)}(\hat{\mathbf{u}}_{I\eta}, \hat{\mathbf{k}}_I), \quad (8)$$

whereas the transition matrix elements have the property

$$S_{l,l';m}^{(p,p')} = (-)^{p-p'} S_{l,l';-m}^{(p,p')}, \quad (9)$$

that is inferred from their explicit expression. Equations (8) and (9) ensure that the scattered field have the correct transformation properties: In fact, the true-vector nature of the electric field requires that it remain unchanged under reflection in the plane of scattering for parallel polarization ( $\eta = 1$ ), whereas it must change its sign for orthogonal polarization ( $\eta = 2$ ). An useful implication of Eqs. (8) and (9) is that the resonances for a given  $\eta$ ,  $p$ , and  $l$  that are associated to  $\pm m$  are degenerate, i. e. they must occur at the same frequency.

We finally emphasize that Eq. (7) presents all the advantages of an approach based on the transition matrix and on the multipole expansion of the fields. Equation (7), in fact, describes the scattering from a particle of given orientation. Nevertheless, by resorting to the transformation properties of the  $W$ -amplitudes under rotation, it is an easy matter to perform analitical averages over the orientation.[13] The averaging procedure, that has been fully discussed elsewhere,[12] yields information on the extinction of a low density dispersion of particles, and thus produces results that can be directly compared with the experimental data.

### 3. Results and discussion

The theory in Section 2 has been applied to the calculation of the extinction spectrum of spheres of MgO with a radius  $\rho_0 = 25$  nm containing a spherical inclusion of Mg with a radius of  $\rho_1 = 16.6$  nm. In other words we are considering a metal sphere coated by its oxide.  $\rho_0$  and  $\rho_1$  were chosen so as to lie within the estimated ranges for the particles in the interstellar medium.[15] Furthermore, our choice implies that the particles, although small, can have resonances also for  $l > 1$ . The dielectric function of Mg was assumed to be of the free-electron Drude form [22]

$$\epsilon = 1 - \frac{\omega_p^2}{\omega(\omega + i\Gamma\omega_p)},$$

where  $\omega_p = 1.6 \cdot 10^{16}$  sec $^{-1}$  and  $\Gamma = 0.01$ . In turn, the dielectric function of MgO was assumed of the damped oscillator form [22]

$$\frac{\epsilon - \epsilon_\infty}{\epsilon_0 - \epsilon_\infty} = \frac{\omega_T^2}{\omega_T^2 - \omega(\omega + i\Gamma\omega_T)},$$

with  $\omega_T = 7.5 \cdot 10^{13}$  sec $^{-1}$ ,  $\Gamma = 0.27$ ,  $\epsilon_0 = 9.8$  and  $\epsilon_\infty = 2.95$ . The results of our calculations are presented by reporting the extinction efficiency

$$Q_\eta = \frac{4}{K\rho_0^2} \text{Im}[f_{\eta\eta}(\hat{\mathbf{k}}_I, \hat{\mathbf{k}}_S = \hat{\mathbf{k}}_I)],$$

as a function of the ratio  $\nu = \omega/\omega_p$ . In the preceding equation  $f_{\eta\eta}(\hat{\mathbf{k}}_I, \hat{\mathbf{k}}_S = \hat{\mathbf{k}}_I)$  is the forward-scattering amplitude for incidence along  $\hat{\mathbf{k}}_I \equiv (\vartheta_I, \varphi_I)$ . Of course when the scatterers are spherically symmetric  $Q_\eta$  is actually independent of the polarization and the index  $\eta$  will, accordingly, be dropped.

In Fig. 2 we report  $Q$  for a sphere of solid Mg with radius  $\rho_1$ . In order to check the convergency of our calculations and to associate the computed resonances to the appropriate value of  $l$ , the extinction efficiency is reported for  $l_M = 1$  and  $l_M = 2$ ,  $l_M$  being the maximum value of  $l$  included in the sums in Eq. (7). We notice that taking  $l_M > 2$  does not cause visible changes on the scale of the figure nor yields the occurrence of any higher order resonance. However, in order to achieve a numerical accuracy to four significant digits all our calculations were actually performed with  $l_M = 5$ . The sphere of Mg presents two resonances: the lowest-frequency peak is associated with  $l = 1$  whereas the second peak is associated with  $l = 2$ . An analysis of the elements of the transition matrix suggests that both peaks are due to electric resonances and, due to the independence of  $m$  of the elements of the transition matrix for a sphere,[21] the value of  $m$  need not be specified. We do not report  $Q$  for the sphere of MgO of radius  $\rho_0$  because this scatterer does not present any resonance in the range of interest.

Our calculations for the actual scatterer were performed with the geometry described in Section 2, for several positions of the inclusion from the centered position to the most

eccentric one, so as to follow the evolution of the resonances as the inclusion becomes more and more eccentric. As one should expect, we found that the effects that are due to the eccentricity achieve the maximum of evidence when the inclusion becomes tangent to the surface of the external sphere so that in the following figures only the results for this extreme case are reported. Accordingly, Fig. 3 shows, for incidence along the  $z$  axis,  $Q_\eta$  for the actual scatterer with the inclusion at maximum eccentricity together with the partial efficiencies

$$q_{\eta l} = \frac{4}{K\rho_0^2} \text{Im}[B_{\eta\eta l}],$$

with  $l = 1, 2$ . Of course, due to the cylindrical symmetry of the scatterer, both the total and the partial extinction efficiencies are independent of  $\eta$ . Figure 3 also reports  $Q$  for the centered inclusion. In the latter case a single electric resonance occurs that is associated to  $l = 1$  whereas the resonance that for a sphere of solid Mg is associated to  $l = 2$  turns out to be so damped as to reduce to a small shoulder. This behavior is easily understood in the framework of the theory of Johnson: [23] On account of the analogy between the radial Schrödinger equation for spherically symmetric systems and the radial Helmholtz equation for spherical scatterers, this author interprets the electromagnetic resonances as quasi-bound states of the radiation within the effective potential well

$$v_l = n^2(r)k^2 - l(l+1)/r^2.$$

The presence of a coating may modify the radial shape of the refractive index  $n(r)$  to such an extent that the potential well for the appropriate value of  $l$  (in the present case for  $l = 2$ ) may not occur at all, thus preventing the occurrence of the corresponding resonance, or may become so shallow as to produce the damping that is observed in Fig. 3. Considerations of this kind do not apply when the inclusion is off center because of the lack of spherical symmetry. Indeed, Fig. 3 shows that when the inclusion is off center the spectrum complicates as four resonances now occur. The one at the lowest frequency is associated to  $l = 1$  and is the evolution of the main peak that occurs when the inclusion is centered. The three further resonances can be attributed to the multiple scattering processes between the inclusion and the external sphere. [13] Due to the off-center position of the inclusion these processes are asymmetric and thus yield the observed multiplication of peaks. The behavior of the quantities  $q_l$  clearly shows that all these peaks arise from the superposition of contributions for  $l = 1$  and  $l = 2$ . The occurrence of this superposition calls for a word of caution about the classification of the resonances into electric and magnetic as well as about the order of the resonating multipoles. In a previous paper [24] we noticed that this classification depends on the origin to which the multipole fields are referred. For a sphere with a centered inclusion there exist a natural origin, namely the center of the external sphere that coincides

with the center of symmetry of the whole scatterer; of course, when the inclusion is eccentric such a center of symmetry does not exist. Now, a multipole field that is purely electric or magnetic when referred to a given origin becomes a superposition of both electric and magnetic multipole fields, in general of all the multiplicities, when referred to a different origin. [25] On the other hand, in the framework of our present approach, the addition theorem of Ref. [25], gives rise to the non-diagonal matrices  $l_{0 \leftarrow 1}$  and  $l_{1 \leftarrow 0}$  in the expression of the transition matrix. As these matrices account for the multiple scattering processes within the components of the scatterer, we feel authorized to state that the high frequency peaks are due to multiple scattering processes and that their electric or magnetic nature cannot be stated in an absolute sense but only with reference to a chosen origin that, in the present case, coincides with the center of the external sphere. With this exception in mind, we can safely state, however, that all the resonances in Fig. 3 belong to  $|m| = 1$  because, for any  $\eta$ ,  $p$ , and  $l$ , the multipole amplitudes  $W_{lm}^{(p)}$  of a plane wave that propagates along the  $z$  axis do not vanish for  $m = \pm 1$  only. Furthermore, according to our remark in Section 2, Eqs. (8) and (9) imply that the resonances associated to  $m$  and to  $-m$  must occur at the same frequency. We finally notice that the same spectrum is obtained by changing the direction of incidence from  $\vartheta_I = 0^\circ$  to  $\vartheta_I = 180^\circ$ : This is an expected result that stems from the symmetry properties of  $f_{\eta\eta}$  for forward scattering. [21]

The results that we presented so far show the expected independence of the polarization either because the scatterer is spherically symmetric, Fig. 2, or because the incidence is along the cylindrical axis, Fig. 3. In this respect let us recall that, according to Eq. (7), the dependence of the scattering amplitude on the polarization as well as on  $\hat{k}_I$  and on  $\hat{k}_S$  is entirely due to the amplitudes  $W$ , that are independent of frequency, however. On the contrary, the possibility of producing resonances is contained in the frequency-dependence of the elements of the transition matrix, that, in turn do not depend either on  $\eta$  or on  $\hat{k}_I$  or on  $\hat{k}_S$ . With this in mind, let us go to discuss the results of Fig. 4 where the dependence of the spectrum on the choice of the polarization shows to its full extent. In Fig. 4, indeed, we superpose to the spectrum for a sphere with a centered inclusion (the same that we reported in Fig. 3) the extinction efficiency for the case of the inclusion at maximum eccentricity for polarization both parallel and perpendicular to the plane of scattering; the direction of incidence is individuated by the polar angles  $\vartheta_I = 52^\circ$ ,  $\varphi_I = 0^\circ$ . This choice of the incidence does not bear any particular significance thus ensuring the true generality of our results. In the same figure we also report the result of the angular average over the particles with the eccentric inclusion on the assumption that they are randomly distributed in orientation; of course, the latter spectrum, that gives information on the extinction from a dispersion of identical scatterers, is independent of the polarization. We first notice that, except for the leftmost peak, all resonances for the case of an eccentric inclusion arise from a

superposition of contributions from  $l = 1$  and for  $l = 2$ ; this is shown by the values of the partial efficiencies  $q_{\eta 1}$  and  $q_{\eta 2}$ , that are not reported, however. Therefore our previous considerations both on the origin and on the classification of the resonances apply. Comparison of the spectra for the individual particles shows that the resonance at  $\nu_1 = 0.535$  occurs only in perpendicular polarization whereas the resonance at  $\nu_2 = 0.545$  occurs only in parallel polarization. The separation  $\nu_2 - \nu_1$ , although small on the scale of the figure, is quite noticeable in wavelength. The peak at  $\nu_1$  is the same that appears in Fig. 3 for  $\vartheta_I = 0^\circ$ . In fact this resonance mainly stems from the elements  $S_{1,1;\pm 1}^{(2,2)}$  that, for  $\vartheta_I = 0^\circ$ , are excited for both polarizations as the relevant amplitudes  $W_{1,\pm 1}^{(2)}$  are independent of the choice of  $\eta$ . On the contrary, for general direction of incidence  $W_{1,\pm 1}^{(2)}$  are unchanged for  $\eta = 2$  whereas they are smaller for  $\eta = 1$ . The peak at  $\nu_2$  originates instead from the leading element  $S_{1,1;0}^{(2,2)}$  that is excited for parallel polarization as the exciting amplitude  $W_{10}^{(2)}$ , provided that the incidence is not along the  $z$  axis, does not vanish for  $\eta = 1$  only.

When the particles are randomly oriented, the averaged spectrum shows that both peaks at  $\nu_1$  and  $\nu_2$  are present. This is an expected result that we already noticed just in connection with the optical properties of spheres containing an eccentric inclusion.[13] Averaging over the orientations, indeed, implies summing the contributions to the extinction efficiency from scatterers whose symmetry axis does not lie, in general, in the plane of scattering. Now, the response of a scatterer with its symmetry axis not lying in the scattering plane is easily recognized as identical to the response of a scatterer with its axis in that plane when this latter object is excited by a wave with an appropriate state of polarization that, in general, is neither parallel nor orthogonal: Therefore the above mentioned response must be a linear combination of the responses for parallel and orthogonal polarization. Since the extinction efficiency of the individual scatterers displays a peak whose frequency changes with the polarization we get the spectrum for random orientation that is reported in Fig. 4. Ultimately, at least one of the resonances of the individual scatterers undergoes evident qualitative changes as a function of the polarization. Thus the appearance of a dependence on the polarization in the resonance spectrum from a dispersion of such particles may provide an indication that a noticeable fraction of them is likely oriented.

#### 4. Conclusion

The results that we presented in section 3 suggest that a careful analysis of the extinction spectrum from spheres containing a spherical inclusion may help establishing whether the inclusion is concentric or eccentric. In the latter case, in fact, the eccentricity yields a multiplicity of resonances that are quite absent in the spectrum from spheres with a centered inclusion. In the case that the inclusion is eccentric, measurements performed

with polarized light may give indication on the fraction of particles that are oriented alike. Getting this kind of information can be of importance e. g. in astrophysics. Indeed, the galactic extinction shows an evident dependence on the polarization for certain lines of sight. This fact has been interpreted as due to the presence of anisotropic particles of the kind we dealt with in this paper which are partially oriented by some magnetic field. Except for the cause of the alignment, that does not concern us here, the results in Section 3 support the reliability of this interpretation.

## References

- [1] P. R. Conwell, C. K. Rushforth, R. E. Benner and S. C. Hill, "Efficient automated algorithm for the sizing of dielectric microspheres using the resonance spectrum," *J. Opt. Soc. Am. A* **1**, 1181–1187 (1984)
- [2] S. C. Hill, C. K. Rushforth, R. E. Benner and P. R. Conwell, "Sizing dielectric spheres and cylinders by aligning measured and computed resonance locations: algorithm for multiple orders," *Appl. Optics* **24**, 2380–2390 (1985).
- [3] J. D. Eversole, H.-B. Lin, A. L. Huston, A. J. Campillo, P. T. Leung and K. Young, "High-precision identification of morphology-dependent resonances in optical processes in microdroplets," *J. Opt. Soc. Am. B* **10**, 1955–1968 (1993).
- [4] D. Q. Chowdhury, S. C. Hill and P. W. Barber, "Morphology-dependent resonances in radially inhomogeneous spheres," *J. Opt. Soc. Am. A* **8**, 1702–1705 (1991).
- [5] R. L. Hightower and C. B. Richardson, "Resonant Mie scattering from layered spheres," *Appl. Optics* **27**, 4850–4855 (1988).
- [6] K. A. Fuller, "Optical resonances of two-sphere systems," *Appl. Optics* **30**, 4716–4731 (1991).
- [7] K. A. Fuller, "Some novel feature of morphology dependent resonances of bispheres," *Appl. Optics* **28**, 3788–3790 (1989).
- [8] G. Videen and P. Chýlek, "Light scattering enhancement and suppression in cylinders and spheres using two coherent plane waves," *Optics Comm.* **98**, 313–322 (1993).
- [9] F. Borghese, P. Denti, R. Saija, E. Fucile and O. I. Sindoni, "Resonance suppression in the extinction spectrum of single and aggregated hemispheres on a reflecting surface," *Appl. Optics* **36** (1997)
- [10] P. C. Waterman, "Symmetry, unitarity and geometry in electromagnetic scattering," *Phys. Rev. D* **3**, 825–839 (1971).
- [11] E. M. Rose, *Multipole Fields* (Wiley, New York, 1955).
- [12] F. Borghese, P. Denti, R. Saija, G. Toscano and O. I. Sindoni, "Macroscopic optical constants of a cloud of randomly oriented nonspherical scatterers," *Nuovo Cim.* **B 81**, 29–50 (1984).
- [13] F. Borghese, P. Denti, R. Saija and O. I. Sindoni, "Optical properties of spheres containing an eccentric spherical inclusion," *J. Opt. Soc. Am. A* **9**, 1327–1335 (1992).
- [14] F. Borghese, P. Denti and R. Saija, "Optical properties of spheres containing several spherical inclusions," *Appl. Opt.* **33**, 484–493 (1994).
- [15] Draine, in *Planets and protostars, II*, D. C. Black and M. Shapley Matthews, eds. (University of Arizona Press, 1985), pp. 621–640.
- [16]

- [17] F. Borghese, P. Denti, R. Saija, G. Toscano and O. I. Sindoni, "Extinction coefficients for a random dispersion of small stratified spheres and a random dispersion of their binary aggregates," *J. Opt. Soc. Am. A* **4**, 1984–1991 (1987).
- [18] J. D. Jackson, *Classical electrodynamics* (Wiley, New York, 1975).
- [19] R. Newton, *Scattering theory of waves and particles* (McGraw-Hill, New York, 1966).
- [20] M. Kerker, *The scattering of light* (Academic Press, New York, 1969).
- [21] H. C. van de Hulst, *Light scattering by small particles* (Wiley, New York, 1957).
- [22] C. Kittel, *Introduction to Solid State Physics* (Wiley, New York, 1976).
- [23] B. R. Johnson, "Theory of morphology-dependent resonances: shape resonances and width formulas," *J. Opt. Soc. Am. A* **10**, 343–352 (1993).
- [24] F. Borghese, P. Denti, R. Saija, G. Toscano and O. I. Sindoni, "Effect of the aggregation on the electromagnetic resonance scattering of dielectric spherical objects," *Nuovo Cim. D* **6**, 545–558 (1985).
- [25] F. Borghese, P. Denti, G. Toscano and O. I. Sindoni, "An addition theorem for vector Helmholtz harmonics," *J. Math. Phys.* **21**, 2754–2755 (1980).

### Figure captions

**Figure 1.** Sketch of the geometry for a sphere with an eccentric inclusion. In actual calculations the center of the inclusion was assumed to lie on the  $z$  axis.

**Figure 2.** Extinction efficiency for a sphere of solid Mg with radius  $\rho_1 = 16.6$  nm. The continuous curve was obtained with  $l_M = 1$  and the dashed curve with  $l_M = 2$ .

**Figure 3.** Extinction efficiency for the actual scatterer with the inclusion centered (continuous curve with dots) and with the inclusion at maximum eccentricity (continuous curve). The dashed and the dotted curves report the partial efficiencies for  $l = 1$  and  $l = 2$ , respectively, for the case of maximum eccentricity. The incidence is along the  $z$  axis ( $\vartheta_I = 0^\circ$ ,  $\varphi_I = 0^\circ$ ).

**Figure 4.** Extinction efficiency for the actual scatterer with the inclusion at maximum eccentricity for polarization parallel (dashed curve) and perpendicular (dotted curve) to the plane of scattering. The incidence is individuated by the polar angles  $\vartheta_I = 52^\circ$ ,  $\varphi_I = 0^\circ$ . The continuous curve reports the extinction efficiency of a dispersion of scatterers with random distribution of the orientations. A detail of the rightmost part of the spectrum is shown in the inset. For comparison the efficiency for the case of the centered inclusion (continuous curve with dots) is also reported.

### Figure captions

**Figure 1.** Sketch of the geometry for a sphere with an eccentric inclusion. In actual calculations the center of the inclusion was assumed to lie on the  $z$  axis.

**Figure 2.** Extinction efficiency for a sphere of solid Mg with radius  $\rho_1 = 16.6$  nm. The continuous curve was obtained with  $l_M = 1$  and the dashed curve with  $l_M = 2$ .

**Figure 3.** Extinction efficiency for the actual scatterer with the inclusion centered (continuous curve with dots) and with the inclusion at maximum eccentricity (continuous curve). The dashed and the dotted curves report the partial efficiencies for  $l = 1$  and  $l = 2$ , respectively, for the case of maximum eccentricity. The incidence is along the  $z$  axis ( $\vartheta_I = 0^\circ$ ,  $\varphi_I = 0^\circ$ ).

**Figure 4.** Extinction efficiency for the actual scatterer with the inclusion at maximum eccentricity for polarization parallel (dashed curve) and perpendicular (dotted curve) to the plane of scattering. The incidence is individuated by the polar angles  $\vartheta_I = 52^\circ$ ,  $\varphi_I = 0^\circ$ . The continuous curve reports the extinction efficiency of a dispersion of scatterers with random distribution of the orientations. A detail of the rightmost part of the spectrum is shown in the inset. For comparison the efficiency for the case of the centered inclusion (continuous curve with dots) is also reported.

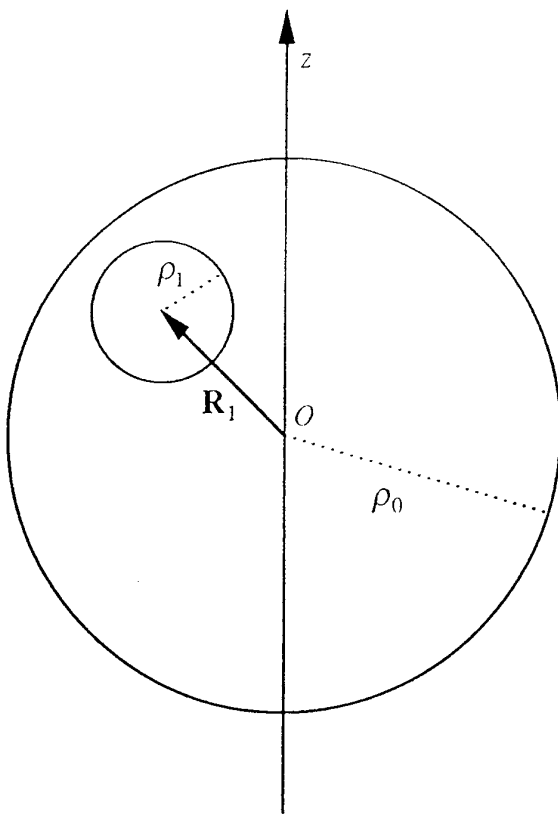


Fig 1

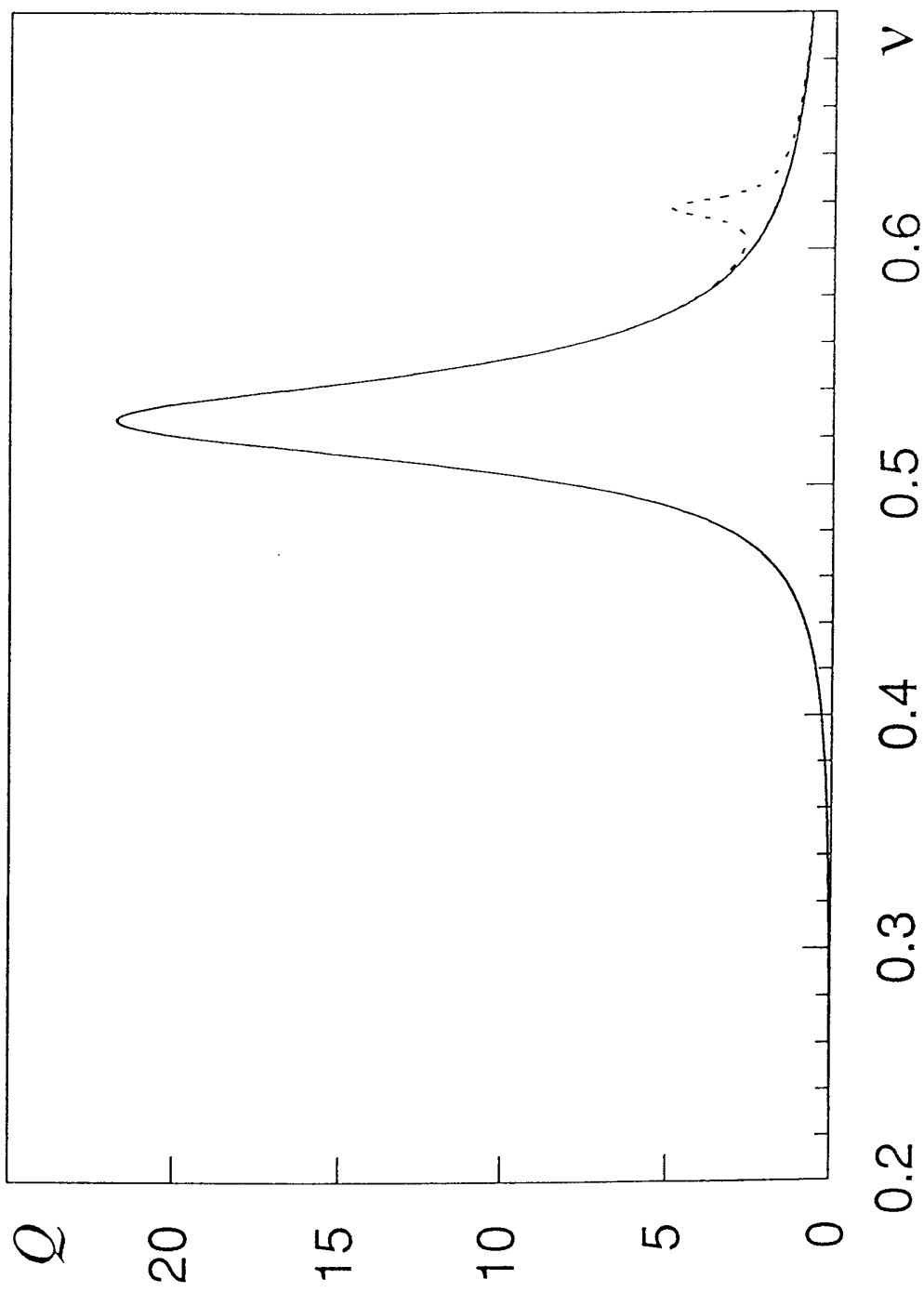


Fig 2

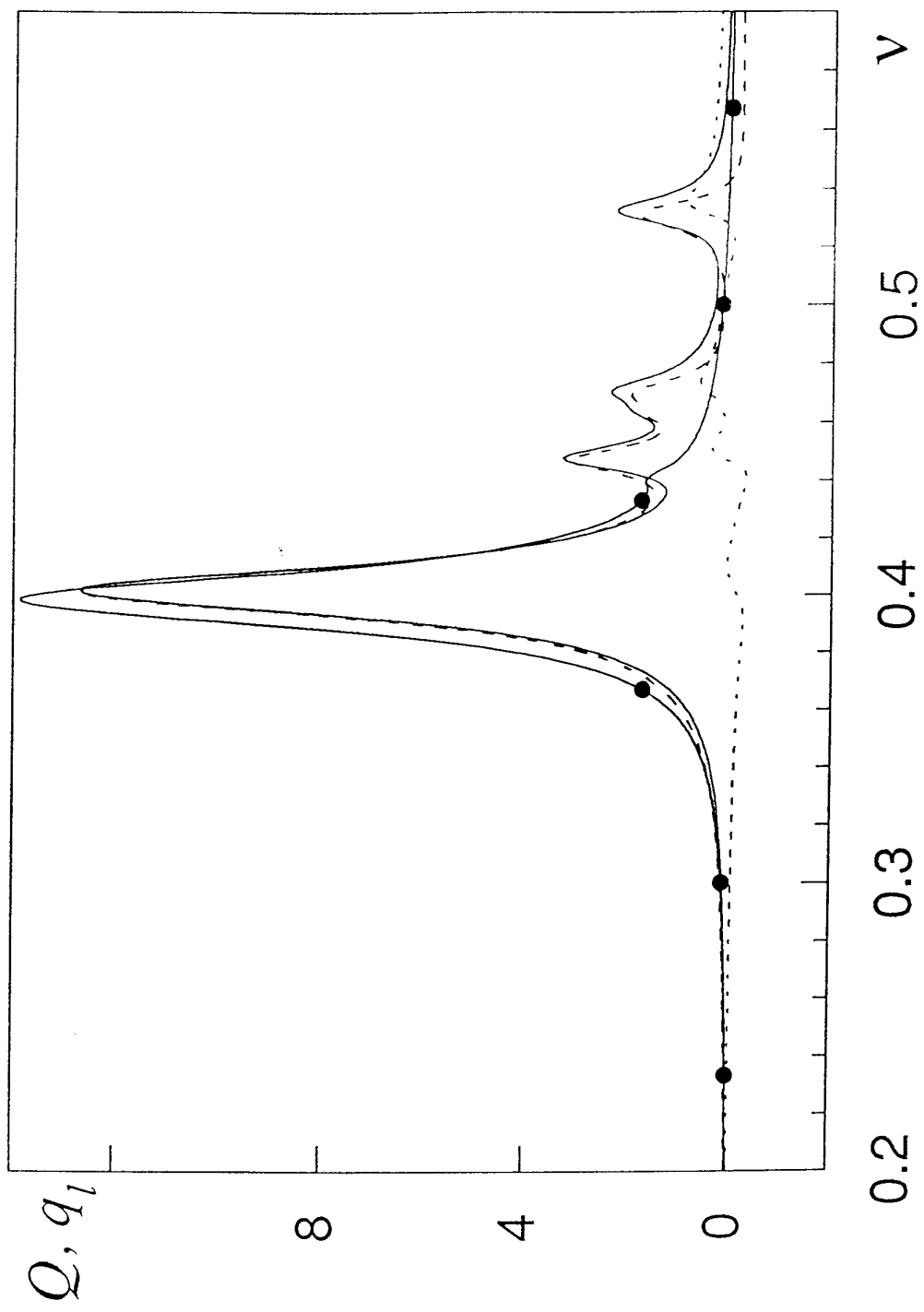


Fig 3

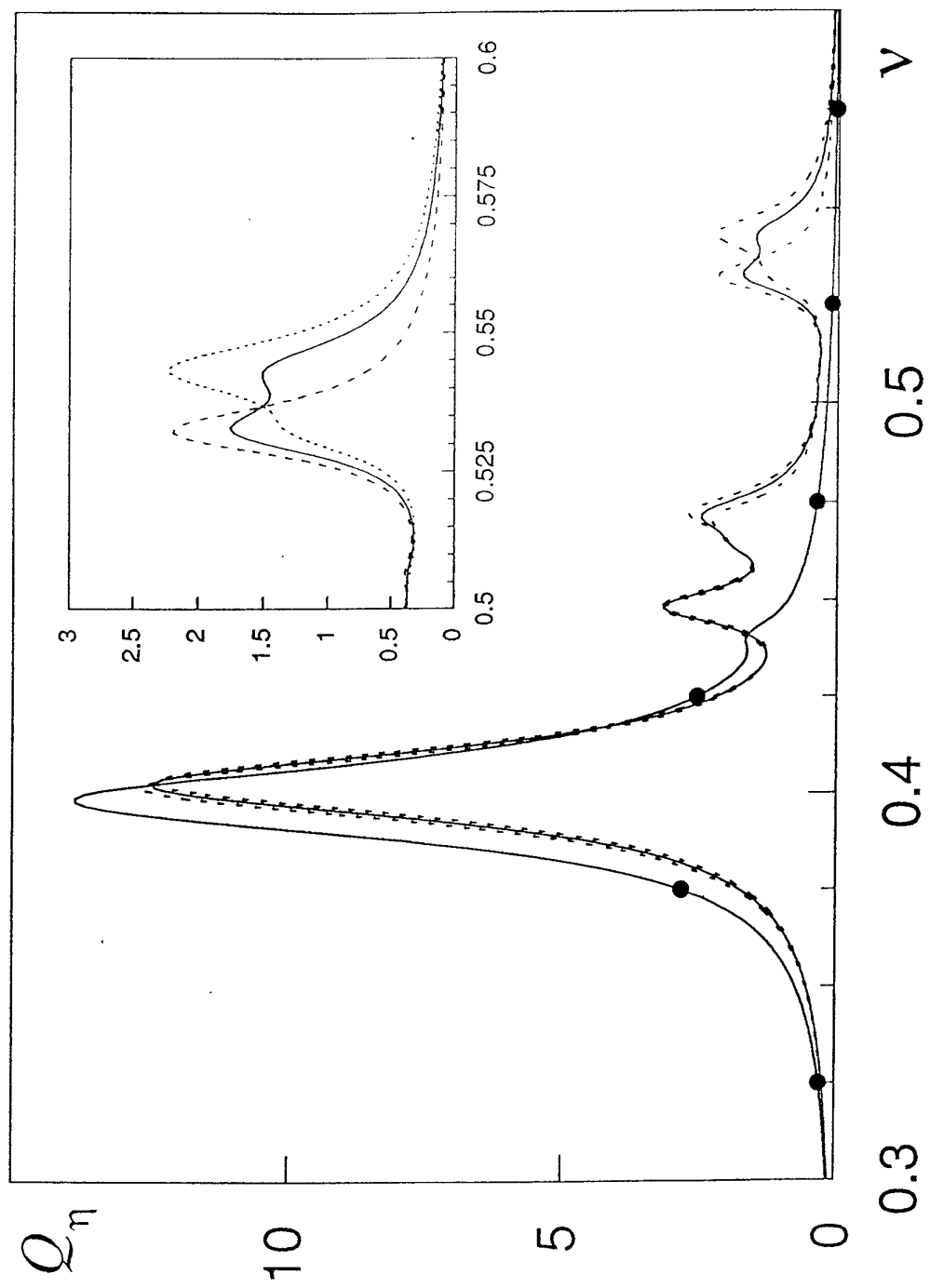


Fig 4